Protein Engineering, Design & Selection vol. 24 no. 4 pp. 385–396, 2011
Published online December 21, 2010 doi:10.1093/protein/gzq118

Combining phage and staphylococcal surface display for generation of ErbB3-specific Affibody molecules

Nina Kronqvist[1,†], Magdalena Malm[1,†], Lovisa Göstring[2], Elin Gunneriusson[3], Martin Nilsson[3], Ingmarie Höidén Guthenberg[3], Lars Gedda[2], Fredrik Y.Frejd[2,3], Stefan Ståhl[1,4] and John Löfblom[1]

[1]Department of Molecular Biotechnology, School of Biotechnology, Royal Institute of Technology (KTH), AlbaNova University Center, SE-106 91 Stockholm, [2]Unit of Biomedical Radiation Sciences, Rudbeck Laboratory, Uppsala University, SE-751 85 Uppsala, Sweden and [3]Affibody AB, Lindhagensgatan 133, SE-112 51 Stockholm, Sweden

[4]To whom correspondence should be addressed.
E-mail: stefans@biotech.kth.se

Received July 29, 2010; revised October 9, 2010; accepted November 18, 2010

Edited by Peter Hudson

Emerging evidence suggests that the catalytically inactive ErbB3 (HER3) protein plays a fundamental role in normal tyrosine kinase receptor signaling as well as in aberrant functioning of these signaling pathways, resulting in several forms of human cancers. ErbB3 has recently also been implicated in resistance to ErbB2-targeting therapies. Here we report the generation of high-affinity ErbB3-specific Affibody molecules intended for future molecular imaging and biotherapeutic applications. Using a high-complexity phage-displayed Affibody library, a number of ErbB3 binders were isolated and specific cell-binding activity was demonstrated in immunofluorescence microscopic studies. Subsequently, a second-generation library was constructed based on sequences of the candidates from the phage display selection. By exploiting the sensitive affinity discrimination capacity of a novel bacterial surface display technology, the affinity of candidate Affibody molecules was further increased down to subnanomolar affinity. In summary, the demonstrated specific targeting of native ErbB3 receptor on human cancer cell lines as well as competition with the heregulin/ErbB3 interaction indicates that these novel biological agents may become useful tools for diagnostic and therapeutic targeting of ErbB3-expressing cancers. Our studies also highlight the powerful approach of combining the advantages of different display technologies for generation of functional high-affinity protein-based binders. Potential future applications, such as radionuclide-based diagnosis and treatment of human cancers are discussed.

Keywords: Affibody/cell surface display/combinatorial protein engineering/HER3/*Staphylococcus carnosus*

Introduction

The epidermal growth factor family of transmembrane tyrosine kinase receptors, including EGFR (ErbB1 or HER1), ErbB2 (HER2), ErbB3 (HER3) and ErbB4 (HER4), are involved in regulating key cellular functions (e.g. cell proliferation, survival, differentiation and migration) through a complex network of intracellular signaling pathways (Citri *et al.*, 2003). Today, it is well established that abnormal expression and signaling of these receptors is associated with development and progression of several forms of cancer, making them important targets for development of novel cancer therapeutics. So far, the EGFR and ErbB2 receptors have been the most extensively studied, with several targeting agents approved by regulatory authorities for diagnosis or treatment of human cancers. Recently, ErbB3 has gained increased attention as the preferred dimerization partner of ErbB2 (Hynes and Lane, 2005; Baselga and Swain, 2009) and together they form a potent oncogenic unit (Holbro *et al.*, 2003). ErbB3 is a key node in activation of the PI3K/Akt pathway promoting tumor cell survival and proliferation (Schoeberl *et al.*, 2009) and is expressed in a number of human cancers, including breast (Bobrow *et al.*, 1997), ovarian (Rajkumar *et al.*, 1996a,b) and bladder cancer (Rajkumar *et al.*, 1996a,b), and plays an important role in signaling in other cancers (Stove and Bracke, 2004), including some lung cancers (Engelman *et al.*, 2005) and prostate cancer (Gregory *et al.*, 2005). Emerging evidence also indicates that the ErbB3 receptor is involved in pre-existing and acquired resistance to ErbB2-directed therapies (Huang *et al.*, 2010; Sergina *et al.*, 2007). In addition, ErbB3 expression has a prognostic value, since high levels of receptor expression are associated with significantly shorter survival time compared with patients that overexpress ErbB2 (Tanner *et al.*, 2006; Reschke *et al.*, 2008).

A relatively large number of the more recently approved therapies directed towards the well-investigated EGFR and ErbB2 receptors are based on monoclonal antibodies. In contrast, there are relatively few reports on the use of anti-ErbB3 antibodies (Baselga and Swain, 2009). To be able to monitor the ErbB3 expression diagnostically *in vivo*, it would be desirable to develop suitable targeting agents that could deliver diagnostic radionuclides for assessment of ErbB3 expression by molecular imaging. Such agents could also mediate a therapeutic effect, either by blocking the receptor/ligand interaction or by using it as a target for delivering a potent payload to the tumor cell.

Although several successful cancer therapy studies have been reported using full-length monoclonal antibodies, this class of agents is not always optimal for targeting solid tumors (both for diagnostic and for therapeutic pay-load purposes). Due to its large size, the IgG molecule has relatively poor tissue penetration capacity (Schmidt and Wittrup, 2009), which can limit efficient distribution of the antibody drug throughout tumors. Additionally, the extraordinarily long *in vivo* half-life of antibodies results in increased blood signals and thereby relatively poor tumor-to-blood contrasts in molecular imaging approaches (Holliger and Hudson, 2005).

[†]These authors contributed equally to this work.

As a response to these specific drawbacks and other limitations associated with the IgG molecule, new scaffolds for protein engineering are being investigated (both antibody derivatives and more recently also non-immunoglobulin protein classes), attempting to address several of these issues (Gebauer and Skerra, 2009; Nygren and Skerra, 2004). One type of such new promising biological agents is the Affibody molecule (Nord *et al.*, 1995; Nord *et al.*, 1997; Nilsson and Tolmachev, 2007; Löfblom *et al.*, 2010), a three-helix bundle protein derived from one of the IgG-binding domains of protein A (Nilsson *et al.*, 1987). The Affibody molecule has several attractive characteristics for a broad range of applications, such as: (i) small size (58 residues), resulting in rapid tissue penetration and enabling solid-phase peptide synthesis for production, (ii) sequence devoid of cysteines, (iii) one of the fastest protein folding kinetics measured (Myers and Oas, 2001) and (iv) high solubility. Thirteen of the solvent accessible residues on helices 1 and 2 have been targeted for randomization in order to build up large combinatorial libraries for subsequent selection of new high-affinity proteins. Affibody molecules with various specificities have been successfully employed in many different settings (Löfblom *et al.*, 2010). For example, the potential use of radiolabeled Affibody molecules in high-contrast radionuclide imaging of cancer biomarkers has already been demonstrated in several pre-clinical and in pilot human clinical studies, using binders with specific affinity for the EGFR (Tolmachev *et al.*, 2009, 2010) and ErbB2 receptor (Tolmachev *et al.*, 2007; Tran *et al.*, 2009; Baum *et al.*, 2010).

Phage display has been the preferred format for generation of Affibody molecules binding to a wide range of targets. However, due to the capture and elution principle of the phage biopanning procedure, fine affinity discrimination is a challenge. This motivates consideration of alternative selection systems for affinity maturation purposes, since affinity improvements in second-generation libraries are generally relatively small. Cell-display systems are emerging as attractive alternatives to phage display for combinatorial protein engineering applications (Daugherty, 2007; Gai and Wittrup, 2007). The larger size of the cell enables the use of fluorescence-activated cell sorting (FACS) for selections from cell-displayed protein libraries while the multivalent display of recombinant proteins (i.e. 10 000–100 000 proteins per cell), together with flow cytometry, offers a quantitative determination of the affinity between the target molecule and individual library members. In addition, the multiparameter analysis enables a real-time measurement of not only the relative affinity for the target molecule, but also the surface expression level of individual protein variants, minimizing undesired expression biases and allowing for fine affinity discrimination between clones (VanAntwerp and Wittrup, 2000; Löfblom *et al.*, 2005).

We have developed an expression system for cell surface display of recombinant proteins on the Gram-positive bacterium *Staphylococcus carnosus* (Samuelson *et al.*, 1995). The system has previously been employed in a wide range of different applications (Wernérus and Ståhl, 2004), and recently we reported a successful selection of TNFα-binding Affibody molecules with high affinity, using a staphylococcal-displayed library (Kronqvist *et al.*, 2008). In addition, using model libraries, we have also demonstrated an extreme fine affinity discrimination capacity of the system, making it particularly well suited for affinity maturation studies (Löfblom *et al.*, 2005).

In this study, we describe a combined strategy for selection and characterization of Affibody molecules specific for the cancer-associated human receptor ErbB3, using both phage and staphylococcal display technologies. Here, phage display was used for selection of first-generation binders from a naïve high-complexity library of randomized Affibody molecules. Based on first-generation sequences, a second-generation affinity maturation library was designed and displayed on staphylococci for subsequent isolation of improved variants using FACS. Characterization revealed several binders with subnanomolar affinity for the human ErbB3 receptor as well as cross-reactivity to murine ErbB3 receptor with low nanomolar affinity. In addition, four clones demonstrated inhibition of binding of the natural ligand heregulin to the receptor, which is potentially valuable for future therapeutic applications. In summary, we here report an efficient strategy for generation of high-affinity ErbB3-specific Affibody molecules using phage display for discovery of binding variants and staphylococcal surface display for affinity optimization and characterization.

Materials and methods

Labeling of ErbB3 and human serum albumin

Biotinylation of recombinant human ErbB3/Fc chimera (R&D Systems, Minneapolis, MN), here denoted ErbB3-Fc, was performed using the Biotin-XX Microscale Protein Labeling Kit (Invitrogen, Carlsbad, CA) according to the supplier's recommendations. The extracellular domain of ErbB3, here denoted ErbB3-ECD, was biotinylated using EZ-Link^{TM}-Sulfo-NHS-LC-LC-Biotin (Pierce, Rockford, IL, USA) according to the supplier's recommendations. Human serum albumin (HSA) was fluorescently labeled using Alexa Fluor 647 succinimidyl ester (Invitrogen) according to the supplier's recommendations. The concentration of labeled proteins was determined using amino acid analysis.

Phage-display selection

A library of random variants of Affibody molecules displayed on bacteriophage, constructed in phagemid pAffi1/pAY00065 as described in Grönwall *et al.* (2007), was used to select ErbB3-ECD-binding Affibody molecules. Preparation of phage stocks from the phagemid library as well as between selections was performed according to previously described procedures (Nord *et al.*, 1997; Hansson *et al.*, 1999) using the helper phage M13K07 (New England Biolabs, Beverly, MA, USA). The *Escherichia coli* amber suppressor strain RR1ΔM15 (Rüther, 1982) was used for all cloning procedures and as host for phage production. The phage selection was performed both in solution as well as selection on solid phase. Unspecific binding of phage particles was minimized by pre-treatment of all tubes and beads with phosphate-buffered saline supplemented with 0.1% Tween 20 and 0.1% gelatin (PBST 0.1). Selection was performed in four cycles. For the selection in solution, four cycles of selection were performed at room temperature (RT) using different concentrations of biotinylated recombinant ErbB3-ECD as target protein. Prior to selection rounds 1 and

2, a preselection step was performed using 100 μg of streptavidin-coated M-280 Dynabeads in order to reduce the amount of streptavidin-binding variants in the library. In cycle 1, phage particles from the Zlib2002 library were incubated with 100 nM of biotinylated ErbB3-ECD in PBST 0.1 gelatin for 2 h. For subsequent cycles, two parallel selection tracks were investigated in which the target concentration was lowered to 50 or 20 nM for cycle 2, 20 or 10 nM for cycle 3 and 20 or 5 nM for cycle 4. The bound phages were captured with streptavidin-coated M-280 Dynabeads (Dynabeads® M-280 Streptavidin, Dynal, Oslo, Norway). For selection on solid phase, MaxiSorp immunotubes (Nunc, Roskilde, Denmark) were immobilized with 1-ml ErbB3-ECD, 10 μg/ml in 50 mM sodium carbonate buffer, pH 9.6 for 1.5 h at RT and thereafter blocked with 3-ml PBST 0.1 gelatin for 1 h at RT. Phage stock was added to the tube and incubated for 2 h. Subsequently, washes were performed twice in cycle 1, three times in cycle 2, six times in cycle 3 and 12 times in cycle 4. The bound phage particles were eluted with 0.1 M glycine–HCl (pH 2.2) followed by immediate neutralization with 1 M Tris–HCl (pH 8). The selection process was monitored by titration of phage stocks before each selection round and after elution from target protein.

ELISA screening for ErbB3-binding activity

In order to screen the isolated Affibody molecules for ErbB3-binding activity, two different ELISA assays were performed, one utilizing biotinylated ErbB3-ECD and the second using ErbB3-Fc as target protein. The ErbB3-specific Affibody molecules (as fusions to an albumin-binding domain derived from streptococcal protein G), as well as an insulin-binding Affibody molecule (Z_{00801}) used as negative control, were prepared as periplasmic supernatants. Protein preparation and ELISA setup was performed as previously described (Friedman *et al.*, 2008). An antibody against human Fc (DAKO, Glostrup, Denmark) labeled with horseradish peroxidase (HRP) and streptavidin-HRP (DAKO) was used for ErbB3-Fc, respectively, ErbB3-ECD detection.

Dot blot analysis

The specificity of first- and second-generation ErbB3-binding Affibody molecules was evaluated by dot blot analysis as previously described (Friedman *et al.*, 2008). The different variants were analyzed against 16 common serum proteins as well as neutravidin, streptavidin, human ErbB2, human ErbB3-ECD, human ErbB3-Fc and ErbB4-Fc. In addition, first-generation binders were analyzed against human ErbB4-ECD, while second-generation Affibody molecules were also analyzed against human EGFR-Fc and human Fc. In case of first-generation binders, periplasmic supernatants were used for blotting while for the second-generation binders purified proteins were utilized.

Expression of soluble Affibody molecules

The genes encoding selected Affibody molecules were subcloned into pAY430, generating dimeric (first-generation binders) or monomeric (second-generation binders) Affibody constructs in fusion with an N-terminal His_6-tag and a C-terminal cysteine for site-specific labeling. Resulting plasmids encoding each Affibody molecule were prepared and transformed into *E. coli* BL21(DE3). Cells were grown in TSB + YE at 37°C until a final OD of ~1 was reached. Protein expression was induced by isopropyl-beta-D-thiogalactopyranoside and cultures were incubated at 25°C for 5 h or overnight. The cells were harvested by centrifugation and the Affibody molecules were purified under denaturing conditions on Ni-NTA Superflow Columns (Qiagen GmbH, Hilden, Germany) or HisPur™ Cobalt resins (Thermo Scientific, Rockford, USA), respectively. Buffer was exchanged to PBS using PD-10 columns (GE Healthcare, Uppsala, Sweden) and for applications using unlabeled His_6-Z-Cys, the C-terminal cysteine was capped with *N*-ethylmaleimide. Prior to capping, the Affibody molecules were reduced in 30 mM DTT for 30 min at 37°C with gentle mixing. DTT was subsequently removed by NAP-10 columns equilibrated with NaAc (0.1 M, pH 6) and *N*-ethylmaleimide was added to the Affibody molecules at 5-fold molar excess and incubated for 1 h at 37°C with gentle mixing. Finally, buffer was exchanged to PBS using NAP-10 columns.

Circular dichroism spectroscopy

Purified ErbB3-binding Affibody molecules were analyzed using circular dichroism (CD) spectroscopy on a Jasco J-810 spectropolarimeter (Jasco Scandinavia AB, Mölndal, Sweden) in a cell with an optical path length of 1 mm. For each Affibody molecule a CD spectrum at 250–195 nm was obtained at 20°C. Thermal unfolding was monitored at a wavelength of 221 nm and a temperature range of 20–90°C (5°C/min).

Immunofluorescence microscopy

The ErbB3 high-expressing human mammary gland cell line, AU565 and ErbB3 low-expressing/ErbB2 high-expressing human ovary carcinoma cell line, SK-OV-3 were cultured as recommended by the provider. The day before assay, 25 000 cells were added to each well of multiwell slides and allowed to grow overnight in a CO_2 incubator. Two experiments were performed. In the first, AU565 cells were stained with 11 different ErbB3-specific Affibody molecules: His_6-$(Z_{01748})_2$-Cys, His_6-$(Z_{01749})_2$-Cys, His_6-$(Z_{01751})_2$-Cys, His_6-$(Z_{01753})_2$-Cys, His_6-$(Z_{01814})_2$-Cys, His_6-$(Z_{01815})_2$-Cys, His_6-$(Z_{01817})_2$-Cys, His_6-$(Z_{01820})_2$-Cys, His_6-$(Z_{01828})_2$-Cys, His_6-$(Z_{01830})_2$-Cys and His_6-$(Z_{02011})_2$-Cys. The second experiment was performed with His_6-$(Z_{01814})_2$-Cys and His_6-$(Z_{01820})_2$-Cys as well as an unrelated Affibody (Z_{01154}) as negative control. The staining was performed on slides with ErbB3 high-expressing AU565 and ErbB3 low-expressing/ErbB2 high-expressing SK-OV-3 cells. An anti-ErbB3 antibody (AF234 Goat-anti-HER3 ab; R&D systems) was included as a positive control in both experiments. The Affibody molecules were added to the wells at a concentration of 15 μg/ml. After 1 h of incubation at RT, the multiwell slides were gently washed and goat anti-Affibody molecule Ig (Affibody AB) was added to each well at a concentration of 5 μg/ml. After 45 min of incubation at RT, the slides were gently washed and chicken anti-goat Alexa Fluor 488 (Invitrogen) at a concentration of 5 μg/ml was added to each well. After an additional 45 min of incubation, the slides were gently washed. The positive control, goat anti-ErbB3 antibody, was used at a concentration of 15 μg/ml followed by 5 μg/ml of chicken anti-goat Alexa Fluor 488. After staining, the cells were fixed in 3% formaldehyde in PBS for 10 min at RT. Slides were then rinsed two times, dried and mounted with anti-fading

solution containing DAPI (4′,6-diamidine-2-phenyl indole, Vector laboratories, Burlingame, CA). The staining was analyzed using a LEICA DMLA microscope equipped with a video camera for live imaging.

On-cell affinity ranking and K_D determination using flow cytometry

The gene sequence encoding Affibody molecules Z_{01751}, Z_{01753}, Z_{01814} and Z_{01820}, respectively, were PCR amplified from their pAY00430 vector constructs and ligated to the staphylococcal display vector pSCZ1. The *E. coli* strain RR1ΔM15 was used as host for plasmid construction and preparation and the constructs were transformed to electrocompetent *S. carnosus* TM300 (Götz, 1990) according to previously described protocol (Löfblom *et al.*, 2007).

Staphylococcal cells displaying the different first- and second-generation Affibody variants, respectively, were inoculated to 10-ml tryptic soy broth supplemented with yeast extract (TSB + YE; Merck, Darmstadt, Germany) and 20-μg/ml chloramphenicol and grown overnight at 37°C and 150 rpm. From ON cultures, ~10^6 cells were washed with 1-ml phosphate-buffered saline supplemented with 0.1% Pluronic® F108 NF Surfactant (PBSP; pH 7.4; BASF Corporation, Mount Olive, NJ). The cells were pelleted by centrifugation (3500 *g*, 4°C, 6 min) and resuspended in 100-μl of PBSP containing different concentrations of biotinylated ErbB3-Fc as well as ErbB2-Fc (100 nM) in case of first-generation binders. Equilibrium binding was reached by incubation at RT for 1 h with gentle mixing. The cells were washed with 1-ml ice-cold PBSP, followed by incubation on ice in 100-μl ice-cold PBSP containing 1.25-μg/ml Streptavidin, Alexa Fluor 488 conjugate (Invitrogen) and 225-nM Alexa Fluor 647, HSA conjugate for 40 min. Following one wash with 1-ml ice-cold PBSP, cells were resuspended in 300-μl ice-cold PBSP prior to flow-cytometric analysis. The mean fluorescence intensity (MFI) was measured using an FACS Vantage SE (BD Biosciences, San Jose, CA) flow cytometer.

Second-generation library construction and cloning

A SlonoMax® library of double-stranded DNA, containing the 131 bp partially randomized helices 1 and 2 of the Affibody sequence 5′-GTA GAT AAC AAA TTC AAC AAA GAA XXX XXX XXX GCG XXX XXX GAG ATC TGG XXX TTA CCT AAC TTA AAC XXX XXX CAA XXX XXX GCC TTC ATC XXX AGT TTA XXX GAT GAC CCA AGC CAA AGC GCT AAC TT-3′ (randomized codons are illustrated as XXX) flanked with restriction sites *Xho*I and *Nhe*I, was ordered from Sloning BioTechnology GmbH (Pucheim, Germany). The library was amplified during eight cycles of PCR followed by PCR purification and restriction enzyme digestion. Ligation of the previously digested staphylococcal display vector pSCZ1 with the randomized library fragments was performed at a 1:4 molar ratio of vector to fragment using T4 DNA ligase (New England Biolabs). The ligation mixture was purified and transformed to electrocompetent *E. coli* DH5α cells. Individual clones, plated directly after transformation as well as after overnight amplification, were PCR amplified for sequence verification using BigDye Thermo Cycle Sequencing reactions and an ABI Prism 3700 instrument (Applied Biosystems, Foster City, CA). Plasmids were prepared and transformed to electrocompetent *S. carnosus* as described previously (Löfblom *et al.*, 2007). The staphylococcal library is hereinafter denoted Sc:$Z_{ErbB3LIB}$.

Cell labeling and FACS

An aliquot of Sc:$Z_{ErbB3LIB}$ (at least 10 times the library size) was inoculated to 100-ml TSB + YE with 20-μg/ml chloramphenicol and grown overnight at 37°C and 150 rpm. After 16 h, cells (at least four times the subsequent sampling number) were labeled with biotinylated ErbB3-Fc, Streptavidin, Alexa Fluor 488 conjugate (Invitrogen) and Alexa Fluor 647 HSA conjugate. Cell labeling and FACS sorting was performed according to previously described procedures (Kronqvist *et al.*, 2008). The cells were sorted in four rounds and after the final round individual clones were sequenced for identification.

Surface plasmon resonance K_D determination

Surface plasmon resonance analysis was performed on a BIAcore™ 2000 instrument (BIAcore AB, Uppsala, Sweden) using PBSP as running buffer at a flow rate of 20-μl/min (unless stated otherwise) and 5 mM NaOH for regeneration. A CM-5 sensor chip (GE Healthcare, Uppsala, Sweden) was immobilized with human ErbB3-Fc (R&D systems) and mouse ErbB3-Fc (R&D systems) by NHS/ECD amine-coupling chemistry. The immobilization of ligands was performed in 10 mM NaAc (pH 4.5) at a flow rate of 30-μl/min and with receptor concentrations of 10 μg/ml, aiming for an immobilization level of 4000 RU.

For determination of the kinetics for respective interaction, 250 μl of four different concentrations (1.5–67 nM diluted in PBSP) of the four second-generation Affibody molecules (Z_{05405}, Z_{05413}, Z_{05416} and Z_{05417}), were injected over the immobilized surfaces of the CM-5 chip. The surfaces were regenerated by four injections of 15 μl of 5 mM NaOH and extensive washing with running buffer. Each sample was measured in duplicates and the response from each Affibody concentration was subtracted with the response from the blank surface. The obtained sensorgrams were fitted to a one-site binding model for determination of K_D values based on mean association (k_{on}) and dissociation rates (k_{off}).

To verify that the Affibody molecules were not selected for the Fc-part of ErbB3-Fc, each Affibody molecule [50 nM] was incubated with a 10-fold molar excess of human polyclonal IgG [500 nM] for 1 h at RT prior to injection of 100 μl of each sample over the biosensor chip immobilized with ErbB3-Fc. In an additional control experiment, the four second-generation Affibody molecules were injected over a sensor chip surface immobilized with ErbB3-ECD.

Competition between heregulin and ErbB3-specific affibody molecules

Competition between the natural ligand heregulin (HRG1-β1 EGF-like domain; R&D systems) and the four ErbB3-specific Affibody molecules for binding to the ErbB3 receptor was analyzed using SPR in two different assays. In the first assay, ErbB3-Fc [2.5 nM] was preincubated with the four ErbB3-specific Affibody molecules [100 nM], respectively, for 1 h at RT, followed by injection of 75 μl of the mixture over a sensor chip immobilized with heregulin (HRG-β1 ECD, R&D systems). In the second assay, co-injections of 100 μl of each Affibody molecule at five

different concentrations (0–10 nM) immediately followed by 100 μl of 250 nM heregulin were performed over the ErbB3-immobilized sensor chip surfaces (i.e. Biacore COINJECT command, resulting in the injection of a second ligand immediately following the first). All samples were injected in duplicates and an ErbB2-specific Affibody molecule was injected using the same setup as a negative control. The surfaces were regenerated with two injections of 5 mM NaOH and extensive washing with running buffer.

Results

Phage-display selection of ErbB3-binding affibody molecules

The previously described phagemid library Zlib2002 (Grönwall *et al.*, 2007), which is based on the 58-residue protein A-derived Z domain (Nilsson *et al.*, 1987), was constructed by NN(G/T) codon degeneracy for randomization of 13 surface-located residues in helices 1 and 2 of the three-helical bundle structure of the domain (Nord *et al.*, 1995; Nord *et al.*, 1997). Zlib2002 was used for phage-display selection of Affibody molecules binding to the ErbB3 receptor. After the fourth round of biopanning, randomly picked clones were subjected to an ELISA screen for detection of ErbB3-binding activity. Independent of selection strategy, ~90% of the clones were positive in the assay, defined as a response 2-fold higher compared with the negative control (data not shown). DNA sequencing, performed on clones with the highest absorbance values from the ELISA, generated 23 unique sequences of which two were considered background binders (Fig. 1A). Sequence homology was observed in several positions, including an entirely conserved tryptophan in position 17. Sequence cluster analysis using average-link hierarchical clustering (Orlova *et al.*, 2006) revealed at least three clusters of binders (data not shown).

Dot blot analysis using periplasmic supernatants

From the ELISA screen, 16 of the 21 unique ErbB3-bindning Affibody molecules (Z_{01748}, Z_{01749}, Z_{01751}, Z_{01753}, Z_{01814}, Z_{01815}, Z_{01816}, Z_{01817}, Z_{01820}, Z_{01821}, Z_{01823}, Z_{01824}, Z_{01826}, Z_{01828}, Z_{01829} and Z_{01830}), representing all three clusters, were selected and investigated using dot blot analysis. In total, 23 different proteins (including ErbB3-ECD and ErbB3-Fc) were blotted onto nitrocellulose membranes. The set of proteins comprised 16 high-abundant human serum proteins as well as the homologous ErbB2 and ErbB4 receptors. The results demonstrated that all Affibody molecules except Z_{01824} bound exclusively to ErbB3-ECD and ErbB3-Fc, indicating specific binding to ErbB3 (data not shown).

CD spectroscopy

In order to further characterize the phage-display isolated binders, 13 Affibody molecules that yielded high expression levels and pure product when produced as dimers with an N-terminal His_6 tag and a C-terminal cysteine, were analyzed using CD spectroscopy. The CD spectrums revealed an α-helical content at 20°C comparable to the parental Z domain, suggesting retained three-helical bundle structure (data not shown).

Immunofluorescence microscopy

Immunofluorescence microscopy was employed for characterization of specificity and binding activity to native ErbB3 expressed on human cancer cell lines. Eleven of the 13 clones investigated using CD spectroscopy, representing all three clusters of binders, were incubated with ErbB3 high-expressing AU565 cells (human mammary gland cell line). Of 11 binders, six clones gave a specific membrane staining pattern and 2 of the ErbB3-specific molecules (Z_{01814} and Z_{01820}) were selected for an additional staining of AU565 cells, which express high levels of ErbB3 and SK-OV-3 cells (human ovary carcinoma cell line), which express high levels of ErbB2, but only low levels of ErbB3. Distinct cell membrane staining was obtained on AU565 but not on SK-OV-3 cells, suggesting specific ErbB3 binding and no cross-reactivity to ErbB2 (Fig. 1B–G).

On-cell affinity ranking using flow cytometry

To further characterize four of the Affibody candidates that showed membrane staining on ErbB3-expressing cells (Z_{01751}, Z_{01753}, Z_{01814} and Z_{01820}) and to verify functional expression on bacterial cells, staphylococcal cell display was employed for an on-cell affinity ranking experiment using flow cytometry. Monomeric constructs of the four variants were subcloned into the staphylococcal display vector for subsequent transformation to the staphylococcal host. Staphylococcal cells displaying the four Affibody molecules in fusion to an albumin-binding protein (ABP, derived from streptococcal protein G), respectively, were incubated with four concentrations of biotinylated ErbB3-Fc ranging from 5 to 100 nM. Cells were analyzed using flow cytometry, revealing efficient expression on the cell surface and specific binding to ErbB3 for all four variants with no significant difference in relative affinity among the clones (data not shown). Biotinylated ErbB2 was used as negative control in the experiments and no cross-specificity was observed, confirming the results from the dot blot and immunofluorescence microscopy experiments.

Affinity maturation library for staphylococcal display

In order to further improve the affinity of the ErbB3-specific Affibody molecules, a second-generation library was designed on basis of the sequences obtained from the phage selection. When designing such affinity maturation libraries, a more restricted diversity is desired, focusing the sequence space around the first-generation clones. However, the traditional oligonucleotide synthesis techniques using mononucleotides and degenerate codons are often limiting the design. Degenerate codons are typically introducing additional unwanted amino acids and stop codons as well as biasing the proportion of amino acids in each position. In this study, a randomized DNA-encoded library was instead generated by the Slonomics® technique, a novel method for incorporation of randomized sets of trinucleotide building blocks during production, providing total freedom when selecting codons during the library design process. The randomization strategy was based on the amino acid composition of the four clones analyzed on staphylococcal cells (Z_{01751}, Z_{01753}, Z_{01814} and Z_{01820}), complemented with consideration of the amino acid distribution for the complete set of phage-selected Affibody binders as well as exclusion of

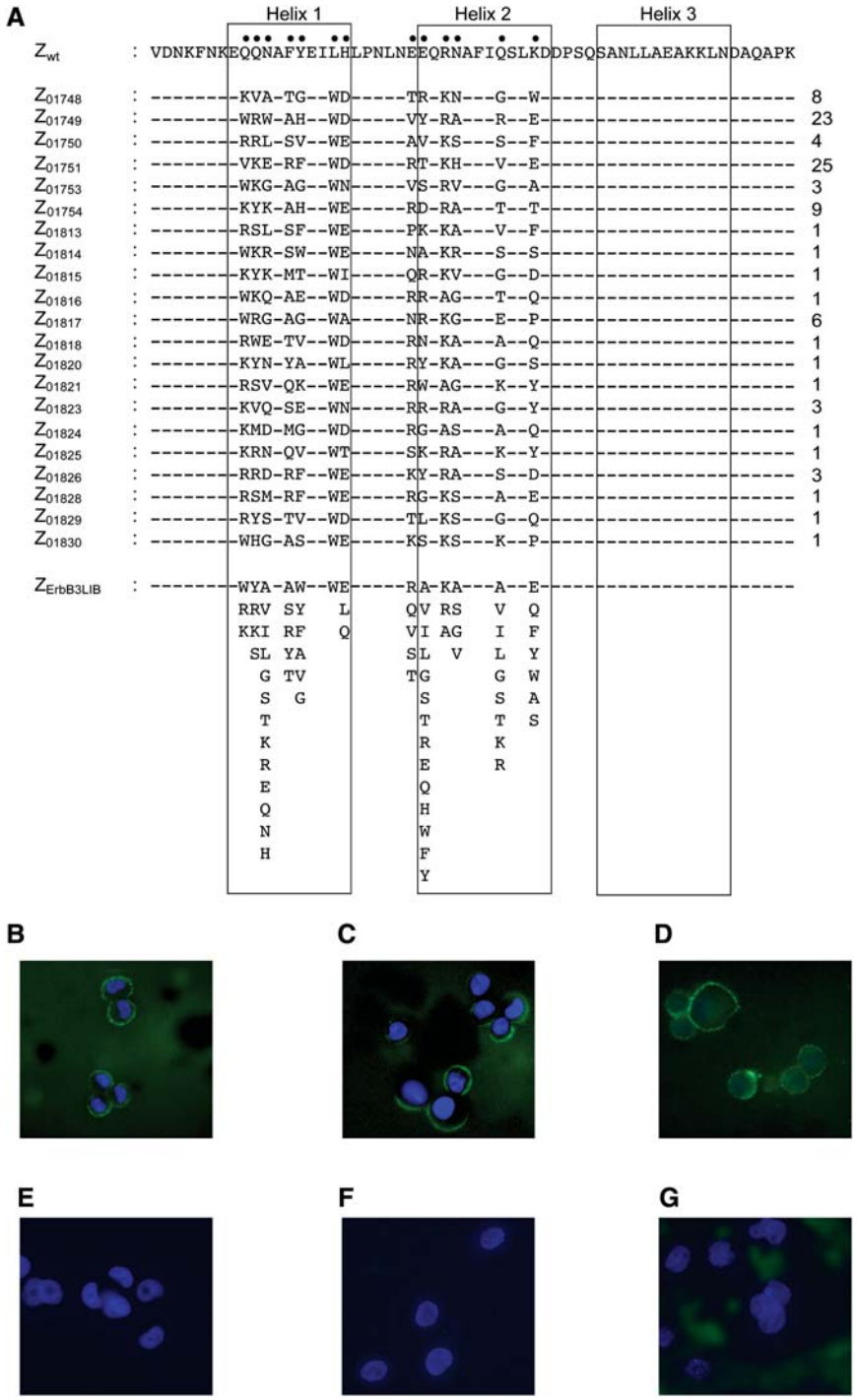

Fig. 1. (**A**) Amino acid sequences (one letter code) of the parental Z_{wt} (with randomized positions indicated with closed circles) and phage-display-selected ErbB3-binding Affibody molecules. Representation among sequenced clones is shown after each sequence. Below the sequences of phage-display-selected Affibody molecules is a schematic overview of the design of the affinity maturation Affibody library ($Z_{ErbB3LIB}$) for staphylococcal display selection showing amino acid representation (one letter code) in 12 randomized positions within helices 1 and 2. Note that position 17 (W) is not randomized in the maturation library. Bottom images: immunofluorescence microscopy image of (**B**) ErbB3-high AU565 cells stained with His6-$(Z_{01814})_2$-cys. (**C**) ErbB3-high AU565 cells stained with His6-$(Z_{01820})_2$-cys. (**D**) ErbB3-high AU565 cells stained with Anti-ErbB3 antibody (positive control). (**E**) ErbB3-high AU565 cells stained with $(Z_{01154})_2$ (negative control). (**F**) ErbB3-low/ErbB2-high SK-OV-3 cells stained with His6-$(Z_{01814})_2$-cys. (**G**) ErbB3-low/ErbB2-high SK-OV-3 cells stained with His6-$(Z_{01820})_2$-cys.

aspartic acid residues in order to avoid aspartimide formation in future chemical peptide synthesis. The Affibody library was randomized in 12 positions within helices 1 and 2 in order to produce a mixture of 7.4×10^8 individual oligonucleotides (Fig. 1A). The library of DNA fragments was cloned into the staphylococcal expression vector and transformed into *S. carnosus* to generate a cell-displayed library containing $\sim 1.3 \times 10^7$ individual clones. Sequence analysis of individual library members revealed a distribution of codons in accordance with the theoretical design and a low proportion of undesired codons, multiple inserts and frame shifts (data not shown). In order to verify that the

Affibody library was functionally displayed on the bacterial surface, staphylococcal cells from the library were incubated with fluorescently labeled HSA and analyzed using flow cytometry. The result showed that around 72% of the library expressed full-length proteins with functional ABP fusions on the cell surface (data not shown), suggesting that the staphylococcal system is indeed a reliable technology for display of recombinant Affibody molecules.

Flow-cytometric sorting for isolation of improved Affibody molecules

For isolation of Affibody molecules with improved affinity for the ErbB3 receptor, the staphylococcal library was subjected to four rounds of fluorescence-activated cell sorting (FACS) with alternating rounds of amplification by cell growth. Briefly, cells were incubated with biotinylated ErbB3 at concentrations around 10-fold lower compared with the estimated K_D of the first-generation binders. Cells were thereafter washed and incubated with fluorescently labeled streptavidin for subsequent fluorescence-mediated detection of cell-bound ErbB3 as well as fluorescently labeled HSA for monitoring of surface expression levels through binding to the ABP expressed in fusion to the Affibody molecules on the surface. The incubation of secondary reagents and HSA was performed on ice in order to reduce the dissociation rate of bound ErbB3. After an additional washing step, the labeled cell library was screened and sorted in a flow cytometer. Selection stringency in terms of target concentration, sorting parameters and sorting gates was increased with each sorting round and typically, the top 0.1% of the library, demonstrating highest target binding to surface expression ratio, was gated and isolated for amplification and subsequent rounds of sorting. One advantage with cell-based selection systems is the straightforward monitoring of the obtained enrichment throughout the selection process, and the visualization of the target-binding properties of the library in the flow cytometer revealed an enrichment of ErbB3-positive clones in each sorting round (Fig. 2). After up to four rounds of FACS, isolated cells were spread on semi-solid medium for sequencing and characterization of individual candidates. The sequencing yielded 443 sequences, out of which 45 clones appeared more than once within the same sorting round (Fig. 3).

On-cell affinity screening and K_D determination of second-generation binders

On the basis of the sequencing results, the 45 clones that appeared multiple times were subjected to a cell-based flow-cytometry assay in order to screen the variants with respect to affinity for ErbB3. Individual clones were incubated with biotinylated ErbB3-Fc and secondary reagents in principle as described above. The staphylococcal cell populations were analyzed using flow cytometry and one of the first-generation binders (Z_{01753}) was included in the analysis for comparison. All 45 candidates were positive for ErbB3 binding in the assay and, moreover, 43 demonstrated a higher signal compared with the first-generation binder (data not shown), indicating an improved affinity for ErbB3. In addition, the four clones that appeared most frequently after sequencing yielded the highest signals in the assay, demonstrating

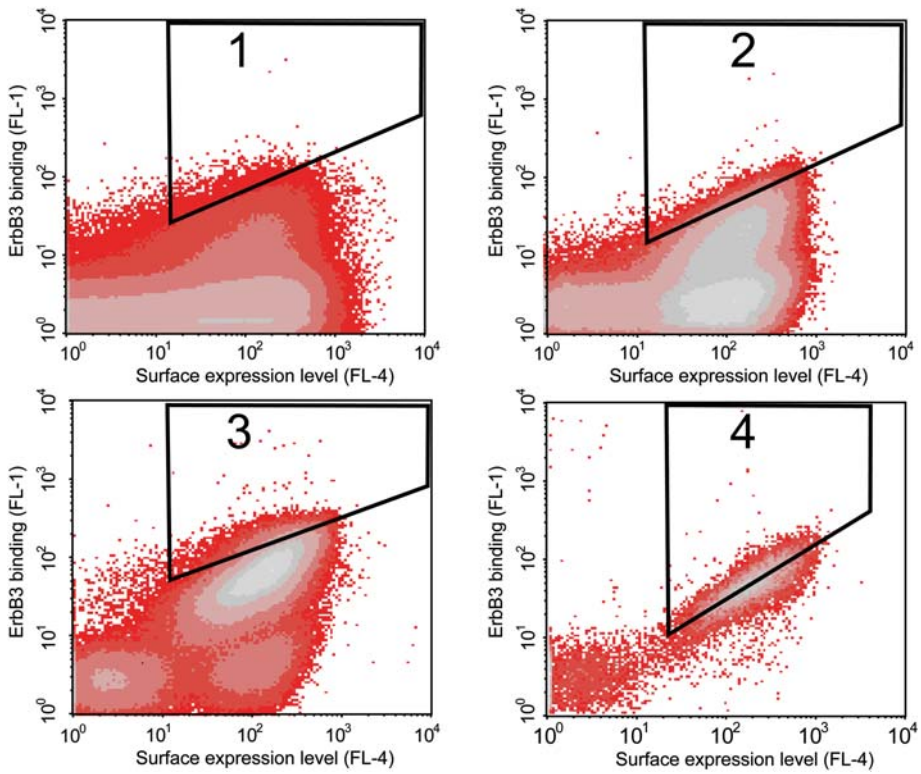

Fig. 2. Density plots showing the results from flow-cytometric sortings of Sc:$Z_{ErbB3LIB}$. FL-4 channel fluorescence intensity corresponding to surface expression level (monitored via HSA binding) on the *x*-axis and FL-1 channel fluorescence corresponding to ErbB3 binding on the *y*-axis. The density plots are showing the staphylococcal library before flow-cytometric sorting of rounds 1, 2, 3 and 4, respectively, with regions used for gating outlined in each plot. Note that the concentration of biotinylated ErbB3-Fc is decreased in each sorting round, resulting in decreasing signal intensities on average in subsequent rounds.

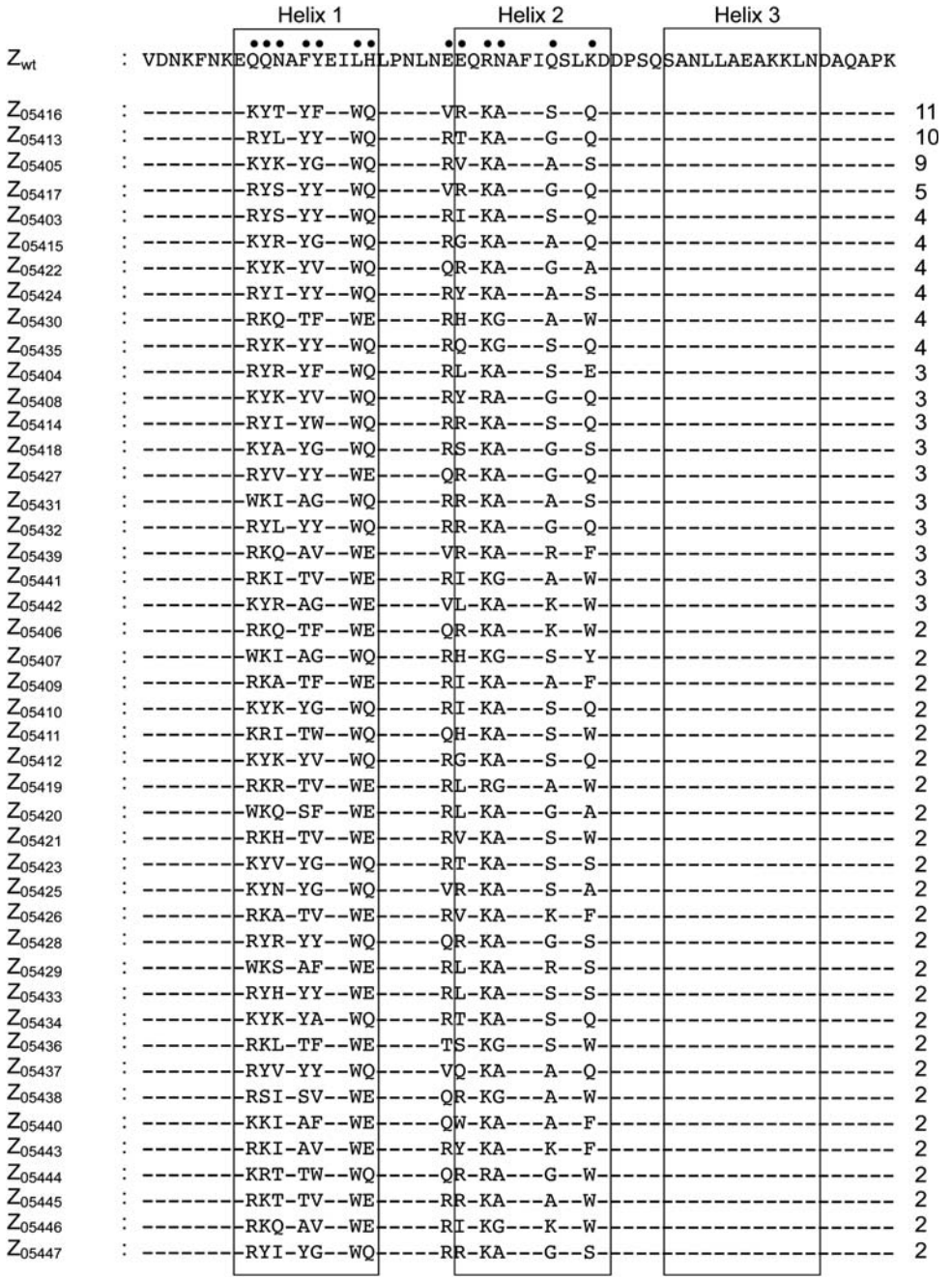

Fig. 3. Amino acid sequences of the parental Z_{wt} with randomized positions indicated with closed circles and FACS-isolated potential ErbB3-binding Affibody molecules. Representation among sequenced clones is shown after each sequence.

quantitative isolation of binders in the flow-cytometric sorting. In order to further characterize the most promising candidates, the apparent equilibrium dissociation constant (K_D) was determined by on-cell analysis for the top four variants (Z_{05405}, Z_{05413}, Z_{05416} and Z_{05417}) and one of the first-generation binders (Z_{01820}). Staphylococcal cells displaying the four variants and the first-generation binder were incubated in varying concentrations of labeled ErbB3 spanning the expected K_D. The cell populations were analyzed in the flow cytometer and the MFI data were subsequently plotted against the ErbB3 concentrations and fitted to a one-site binding model in order to determine the apparent K_D. All four second-generation binders demonstrated low nanomolar affinity and for the strongest binder an improvement of affinity of around 15-fold compared with the first-generation binder (Fig. 4, Table I).

CD spectroscopy

CD spectroscopy was used to determine the secondary structure content as well as the thermal stability of the four affinity-matured ErbB3-binders. Purified Affibody molecules were subjected to polarized light, generating CD spectra that indicated retained α-helical structure for all four molecules (Fig. 5A). Melting temperatures were determined, ranging from 52°C to 61°C (Fig. 5B, Table I). Additionally, refolding of the α-helical structure subsequent to the heat treatment was shown to be complete in all four cases (Fig. 5A).

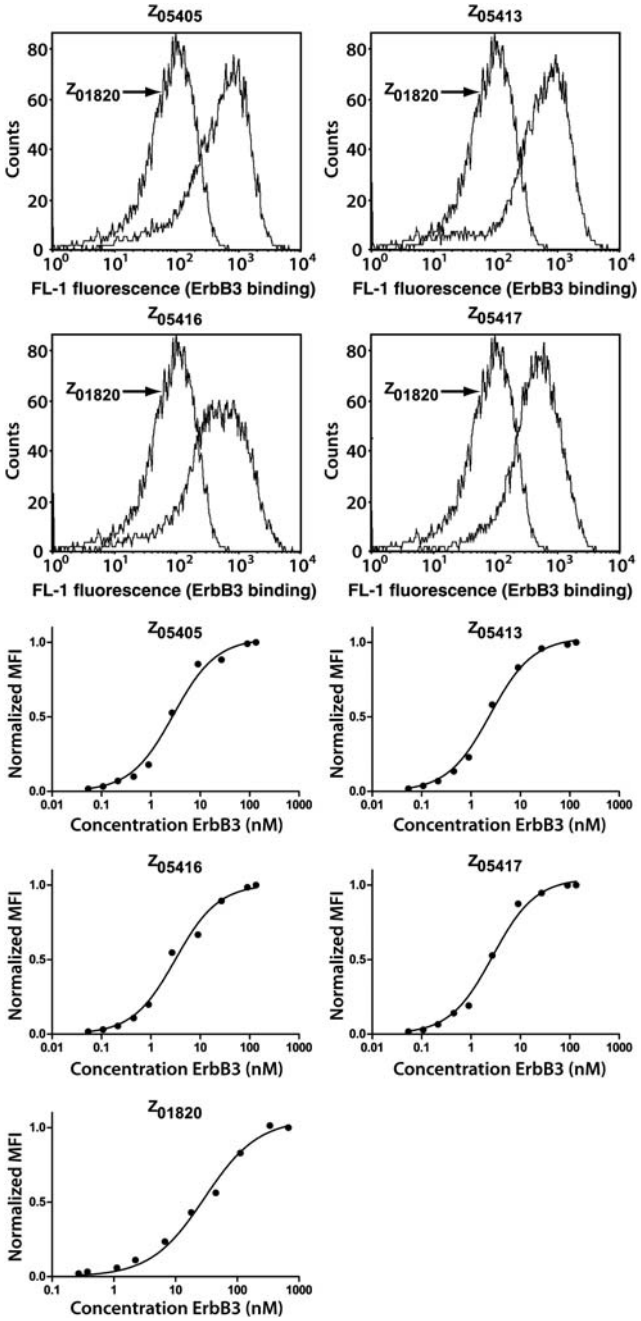

Fig. 4. (**A**) Histograms from flow-cytometric analysis of ErbB3 binding of staphylococcal cells displaying the four ErbB3-specific Affibody molecules (Z_{05405}, Z_{05413}, Z_{05416} and Z_{05417}), respectively. Overlay from analysis of cells displaying the first generation binder Z_{1820} is included in each histogram for comparison. Cells were incubated in 3 nM-labeled ErbB3-Fc prior to analysis. FL-1 channel fluorescence corresponding to ErbB3-Fc-binding on the *x*-axis and cell counts on the *y*-axis. (**B**) On-cell flow-cytometric determination of the apparent equilibrium dissociation constant (K_D) for four ErbB3-specific Affibody molecules (Z_{05405}, Z_{05413}, Z_{05416} and Z_{05417}) from the bacterial surface display selection and one ErbB3-specific Affibody molecule (Z_{01820}) from the phage-display selection. Representative binding isotherms with the normalized MFI on the *y*-axis and the biotinylated ErbB3-Fc concentration on the *x*-axis. The MFI is normalized with the MFI for the cell population incubated with the highest concentration of biotinylated ErbB3-Fc in each experiment. Solid line represents the equation from fitting the data to a one-site binding model.

Surface plasmon resonance K_D determination

The dissociation equilibrium constant (K_D) of the four second-generation Affibody molecules was determined by surface plasmon resonance technology. Four different concentrations (1.5–67 nM) of respective Affibody molecules were injected over sensor chip surfaces immobilized with human ErbB3-Fc and mouse ErbB3-Fc, respectively. The affinity was determined from the association and dissociation rates of the Affibody molecules using non-linear regression to a one-site binding model, resulting in dissociation constants of 1.61 nM for Z_{05405}, 0.78 nM for Z_{05413}, 0.78 nM for Z_{05416} and 0.69 nM for Z_{05417} (Fig. 5C, Table I). Since the sorting of second-generation ErbB3 binders was performed with ErbB3 fused to the human IgG Fc-region, two control experiments were performed in order to verify that the Affibody molecules were not selected for the Fc-part. In the first assay, the Affibody variants were pre-incubated with a 10-fold molar excess of human polyclonal IgG prior to injection over the sensor chip surface. No difference in response was observed for Affibody molecules pre-incubated with IgG compared with samples containing only Affibody molecules (data not shown). In the second assay, the Affibody molecules were injected over a surface with ErbB3-ECD, showing specific binding for all four binders (data not shown). Taken together, the two experiments clearly demonstrate that Fc is not part of the Affibody binding site on ErbB3-Fc.

Dot blot analysis of second-generation Affibody molecules

The specificity of the affinity-matured Affibody molecules was analyzed in a dot blot assay against 24 different proteins, including human EGFR-Fc, ErbB2-Fc, ErbB3-Fc and ErbB4-Fc. Z_{05405}, Z_{05413}, Z_{05416} and Z_{05417} all bound to ErbB3-Fc but not to the other homologous ErbB receptors, the Fc domain or the serum proteins, indicating specific interaction with the extracellular domain of ErbB3 (data not shown). Although binding of all four affinity-matured Affibody molecules to ErbB3-ECD was demonstrated using Biacore, binding to ErbB3-ECD was not detectable in the dot blot assay (possibly due to decreased integrity of ErbB3-ECD when spotted on the membrane). A Taq polymerase-specific Affibody molecule was employed as a negative control in the assay, showing no binding to any of the 24 proteins (data not shown).

Surface plasmon resonance competition assay

The high sequence homology of the four Affibody molecules from the affinity maturation, suggests that they all recognize the same epitope on ErbB3. For potential therapeutic applications of the ErbB3-specific Affibody molecules, competition with the natural ErbB3 ligand heregulin for binding to ErbB3 would be valuable. A competition study using surface plasmon resonance technology was therefore performed. Heregulin was immobilized on the Biacore chip surface and ErbB3-Fc was preincubated with 40-fold molar excess of the four affinity-matured Affibody molecules, respectively, and subsequently injected over the heregulin surface. The results showed a nearly complete reduction in the response level compared with injecting ErbB3-Fc not preincubated with Affibody molecules (Fig. 6A). To verify the results, a similar SPR study was performed using ErbB3-Fc immobilized on the chip surface. Various concentrations of the second-generation Affibody molecules were injected immediately followed by injection of the EGF-like domain of heregulin over the ErbB3-surfaces. As a negative control, the

Table I. Affinities of five Affibody molecules for human/mouse ErbB3 and melting temperatures

	Human ErbB3				Mouse ErbB3			
	On-cell analysis	Biosensor analysis			Biosensor analysis			
Clone	$K_{D,\ app}$ (nM)[a]	K_D (nM)[b]	k_a (M^{-1} s^{-1})[b]	K_D (s^{-1})[b]	K_D (nM)[b]	k_a (M^{-1} s^{-1})[b]	K_D (s^{-1})[b]	T_m (°C)
Z_{05405}	2.5	1.6	1.8×10^6	2.8×10^{-3}	2.4	1.4×10^6	3.3×10^{-3}	52
Z_{05413}	1.8	0.8	1.7×10^6	1.3×10^{-3}	2.0	1.4×10^6	3.0×10^{-3}	55
Z_{05416}	2.9	0.8	1.9×10^6	1.5×10^{-3}	2.0	1.6×10^6	3.2×10^{-3}	61
Z_{05417}	3.0	0.7	1.9×10^6	1.3×10^{-3}	1.7	1.6×10^6	2.7×10^{-3}	57
Z_{01820}	30.2	ND	ND	ND	ND	ND	ND	ND

[a]Mean of duplicates performed on different days using freshly prepared dilutions.
[b]Mean of duplicates of each concentration performed on the same day.

ErbB2-specific Affibody was co-injected with heregulin in the same manner. The results indicated a concentration-dependent competition with the interaction between the ErbB3 receptor and its natural ligand (Fig. 6B). The same was observed for mouse ErbB3-Fc (data not shown). No competition between the negative control and heregulin could be observed for either human or mouse ErbB3 (data not shown). The results demonstrate that the selected Affibody molecules interact with the same binding site on ErbB3 as the natural ligand heregulin and can hence compete with the binding between the ligand and the receptor *in vitro*, suggesting a potential therapeutic effect in future *in vivo* applications.

Discussion

Targeting transmembrane tyrosine kinase receptors overexpressed on tumor cells using specific affinity proteins (e.g. monoclonal antibodies) is an efficient strategy to diagnose or treat various cancer diseases, as reported in several recent studies. We have previously demonstrated promising results using two distinct Affibody molecules specific for the EGFR and ErbB2 receptor, respectively, for such purposes. Here we have investigated the potential of combining two different display technologies for generation of Affibody molecules targeting the related ErbB3 receptor. Traditional phage-display technology was used for initial discovery of new affinity proteins with specific ErbB3-binding properties and staphylococcal surface display was subsequently used for affinity maturation and on-cell characterization of isolated second-generation candidates. The phage-display selections yielded in total 21 unique binders with confirmed affinity for ErbB3. Although homology analysis of the sequences revealed at least three clusters of binders, the sequences were related with a conserved tryptophan residue in position 17 for all Affibody molecules. Since recombinant soluble receptor protein was used as target in the selections, an immunofluorescence microscopic analysis was used to verify specific binding to native ErbB3 receptor expressed on a cancer cell line. The affinity of four phage-display selected binders was thereafter estimated using on-cell flow-cytometric analysis to around 10–100 nM. Although not always crucial, the affinity is an important trait in many downstream applications and a maturation effort was hence initiated in order to increase the affinity even further. Since cell display has been reported to work particularly well for optimization of affinity with reported improvements up to 200 000-fold (Jin *et al.*, 2006), an in-house developed staphylococcal system was employed for this purpose. On the basis of generated sequences from the phage-display selection, an Affibody library was constructed using a new technology for trinucleotide-based production of randomized double-stranded DNA. Compared to designing the library for traditional mononucleotide-based synthesis and degenerate codons, employing the Slonomics trinucleotide-based technology resulted in a dramatically improved design. In summary, stop codons in six positions, helix-breaking prolines in three positions and cysteines in four positions, could be avoided. Moreover, again in comparison to mononucleotide synthesis, the theoretical library size was decreased around 3750-fold given that no additional unwanted codons were introduced, resulting in a considerably better coverage and hence a potentially higher functionality of the final cell-displayed library. The flow-cytometric sorting of the cell displayed Affibody library provided straightforward isolation of improved variants with control over the sorting process and direct feedback regarding the enrichment in each cycle. In addition, after isolation, affinity of isolated binders for ErbB3 was readily verified in a cell-based assay. The affinity was later determined using SPR technology to subnanomolar affinity, in total an improvement of at least 15-fold compared with first-generation Affibody molecules from the phage-display selection.

While speculating if this is sufficient for the intended *in vivo* applications, it should be noted that the affinity is higher compared with previously generated binder against the EGFR receptor (Friedman *et al.*, 2008). The EGFR-specific Affibody has been evaluated in preclinical studies for potential radionuclide imaging of tumors and a ^{111}In-labeled form of the binder demonstrated a tumor-to-blood ratio of 100 ± 19 (24 h p.i.; Tolmachev *et al.*, 2009), suggesting a potential for these new ErbB3-specific variants as well.

The second-generation binders also demonstrated blocking of the ErbB3 receptor/heregulin interaction *in vitro*, indicating that the ErbB3-specific Affibody molecules might even potentially be used in future therapeutic applications, either alone as a blocking agent or conjugated to various cytotoxic payloads, such as radionuclides, small molecular drugs or toxins.

Dimerization of an affinity protein in order to increase affinity by the avidity effect is a straightforward approach reported in numerous publications. However, in addition to constructing homodimers of the ErbB3-binding Affibody,

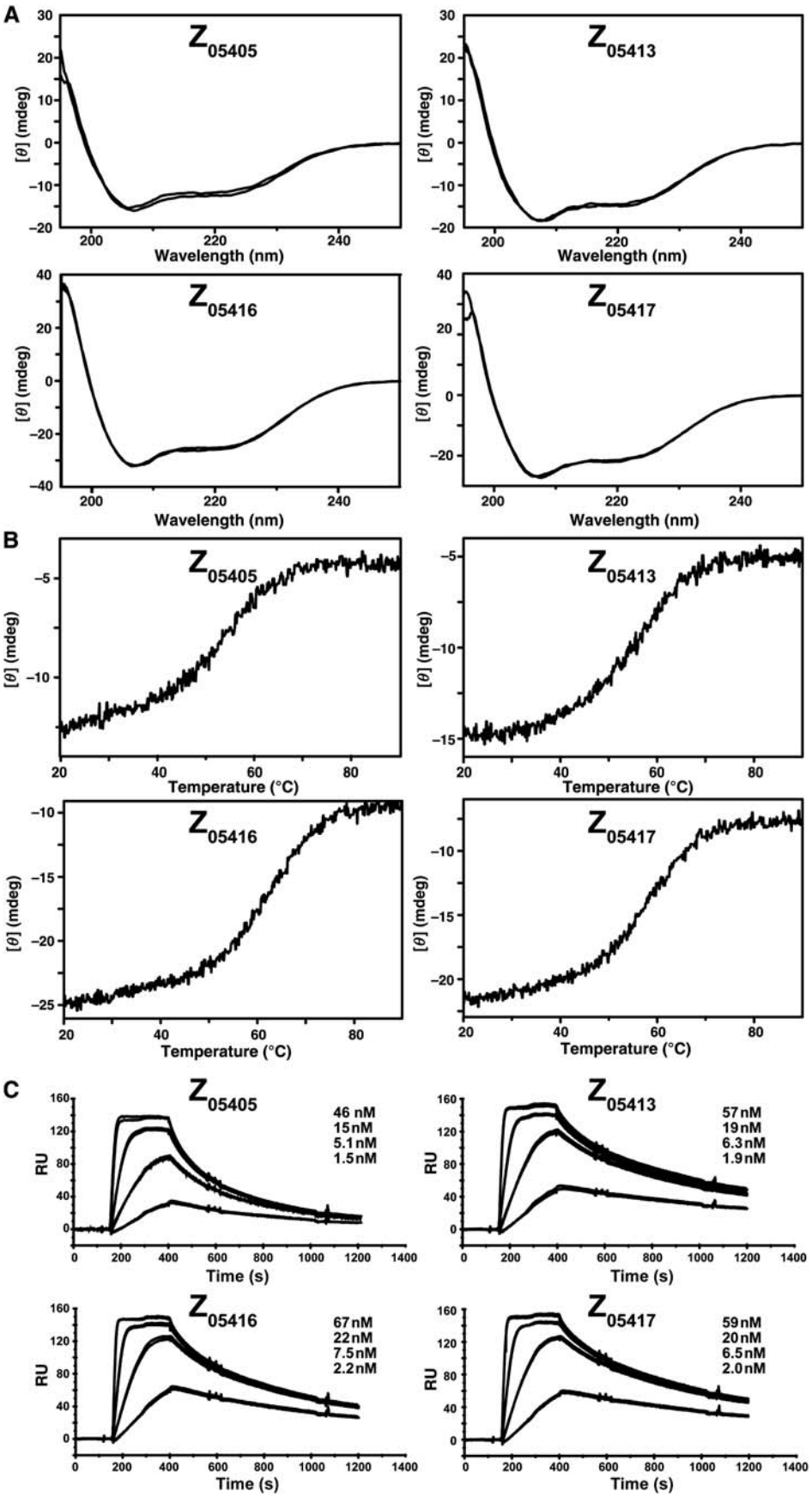

Fig. 5 Secondary structure content, thermal stability and SPR kinetic analysis of Z_{05405}, Z_{05413}, Z_{05416} and Z_{05417}. (**A**) CD spectrum of the four Affibody molecules, before and after heating to 90°C. (**B**) Variable temperature CD spectra generated by heat treatment from 20 to 90°C for the four Affibody molecules. (**C**) Sensorgrams obtained from surface plasmon resonance kinetic analysis, showing four different concentrations of the four Affibody molecules injected over a surface immobilized with human ErbB3-Fc. Dissociation constants were determined based on k_{on} and k_{off} generated by fitting the data to a one-site binding model. Concentrations of injected Affibody molecules are shown in the figure.

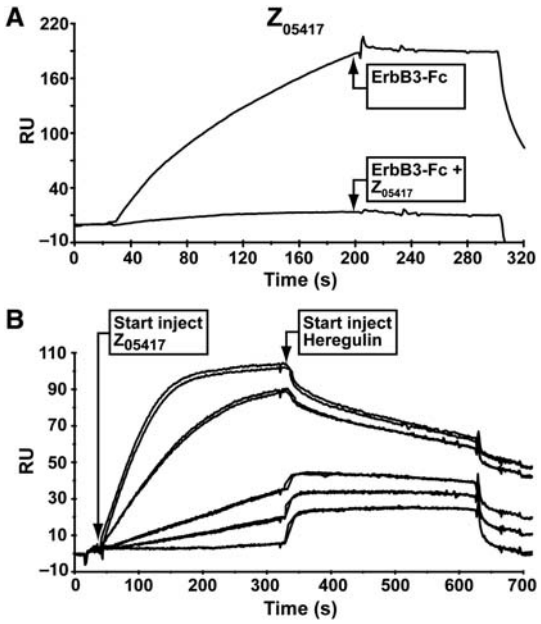

Fig. 6 (**A**) Representative SPR sensorgram from competition analysis of Z_{05417} with heregulin. Sensorgram showing injections of ErbB3-Fc, either alone or preincubated with 40-fold molar excess of Affibody molecule, over a surface immobilized with human heregulin. (**B**) Representative SPR sensorgram from competition analysis of Z_{05417} with heregulin. Sensorgram showing Affibody molecule coinjected in individual duplicates with the ErbB3 ligand heregulin over a surface immobilized with human ErbB3-Fc (i.e. Biacore COINJECT command, resulting in the injection of a second ligand immediately following the first). Each Affibody was injected in five concentrations (10, 5, 1, 0.5 and 0 nM), followed by injection of heregulin (250 nM).

another interesting strategy would be to fuse it to the high-affinity anti-ErbB2 Affibody in order to build bispecific heterodimers. Since ErbB2 and ErbB3 is a particularly potent heterodimerization pair and oncogenic unit in many cancer forms, the bispecific approach could be a way forward to block this interaction or to even potentially further increase specificity for tumors overexpressing both ErbB2 and ErbB3. A proof-of-principle study, demonstrating the potential of a bispecific system containing an EGFR and ErbB2-binding Affibody was recently published (Friedman *et al.*, 2009).

Funding

This work was supported by the Swedish Research Council (VR) [2009-5758], the VINNOVA excellence center for protein technology (Pronova) and VINNOVA [2008-00143, SAMPOST].

References

Baselga,J. and Swain,S.M. (2009) *Nat. Rev. Cancer*, **9**, 463–475.
Baum,R.P., Prasad,V., Muller,D., Schuchardt,C., Orlova,A., Wennborg,A., Tolmachev,V. and Feldwisch,J. (2010) *J. Nucl. Med.*, **51**, 892–897.
Bobrow,L.G., Millis,R.R., Happerfield,L.C. and Gullick,W.J. (1997) *Eur. J. Cancer*, **33**, 1846–1850.
Citri,A., Skaria,K.B. and Yarden,Y. (2003) *Exp. Cell Res.*, **284**, 54–65.
Daugherty,P.S. (2007) *Curr. Opin. Struct. Biol.*, **17**, 474–480.
Engelman,J.A., Janne,P.A., Mermel,C., Pearlberg,J., Mukohara,T., Fleet,C., Cichowski,K., Johnson,B.E. and Cantley,L.C. (2005) *Proc. Natl Acad. Sci. USA*, **102**, 3788–3793.
Friedman,M., Orlova,A., Johansson,E., Eriksson,T.L., Höidén-Guthenberg,I., Tolmachev,V., Nilsson,F.Y. and Ståhl,S. (2008) *J. Mol. Biol.*, **376**, 1388–1402.
Friedman,M., Lindström,S., Ekerljung,L., Andersson-Svahn,H., Carlsson,J., Brismar,H., Gedda,L., Frejd,F.Y. and Ståhl,S. (2009) *Biotechnol. Appl. Biochem.*, **54**, 121–131.
Gai,S.A. and Wittrup,K.D. (2007) *Curr. Opin. Struct. Biol.*, **17**, 467–473.
Gebauer,M. and Skerra,A. (2009) *Curr. Opin. Chem. Biol.*, **13**, 245–255.
Götz,F. (1990) *Soc. Appl. Bacteriol. Symp. Ser.*, **19**, 49S–53S.
Gregory,C.W., Whang,Y.E., McCall,W., Fei,X., Liu,Y., Ponguta,L.A., French,F.S., Wilson,E.M. and Earp,H.S., III (2005) *Clin. Cancer Res.*, **11**, 1704–1712.
Grönwall,C., Jonsson,A., Lindström,S., Gunneriusson,E., Ståhl,S. and Herne,N. (2007) *J. Biotechnol.*, **128**, 162–183.
Hansson,M., Ringdahl,J., Robert,A., Power,U., Goetsch,L., Nguyen,T.N., Uhlén,M., Ståhl,S. and Nygren,P.Å. (1999) *Immunotechnology*, **4**, 237–252.
Holbro,T., Beerli,R.R., Maurer,F., Koziczak,M., Barbas,C.F., III and Hynes,N.E. (2003) *Proc. Natl Acad. Sci. USA*, **100**, 8933–8938.
Holliger,P. and Hudson,P.J. (2005) *Nat. Biotechnol.*, **23**, 1126–1136.
Huang,X., Gao,L., Wang,S., McManaman,J.L., Thor,A.D., Yang,X., Esteva,F.J. and Liu,B. (2010) *Cancer Res.*, **70**, 1204–1214.
Hynes,N.E. and Lane,H.A. (2005) *Nat. Rev. Cancer*, **5**, 341–354.
Jin,M., Song,G., Carman,C.V., Kim,Y.S., Astrof,N.S., Shimaoka,M., Wittrup,D.K. and Springer,T.A. (2006) *Proc. Natl Acad. Sci. USA*, **103**, 5758–5763.
Kronqvist,N., Löfblom,J., Jonsson,A., Wernérus,H. and Ståhl,S. (2008) *Protein Eng. Des. Sel.*, **21**, 247–255.
Löfblom,J., Wernérus,H. and Ståhl,S. (2005) *FEMS Microbiol. Lett.*, **248**, 189–198.
Löfblom,J., Kronqvist,N., Uhlén,M., Ståhl,S. and Wernérus,H. (2007) *J. Appl. Microbiol.*, **102**, 736–747.
Löfblom,J., Feldwisch,J., Tolmachev,V., Carlsson,J., Ståhl,S. and Frejd,F.Y. (2010) *FEBS Lett.*, **584**, 2670–2680.
Myers,J.K. and Oas,T.G. (2001) *Nat. Struct. Biol.*, **8**, 552–558.
Nilsson,F.Y. and Tolmachev,V. (2007) *Curr. Opin. Drug Discov. Devel.*, **10**, 167–175.
Nilsson,B., Moks,T., Jansson,B., Abrahmsén,L., Elmblad,A., Holmgren,E., Henrichson,C., Jones,T.A. and Uhlén,M. (1987) *Protein Eng.*, **1**, 107–113.
Nord,K., Nilsson,J., Nilsson,B., Uhlén,M. and Nygren,P.Å. (1995) *Protein Eng.*, **8**, 601–608.
Nord,K., Gunneriusson,E., Ringdahl,J., Ståhl,S., Uhlén,M. and Nygren,P.Å. (1997) *Nat. Biotechnol.*, **15**, 772–777.
Nygren,P.Å. and Skerra,A. (2004) *J. Immunol. Methods*, **290**, 3–28.
Orlova,A., Magnusson,M., Eriksson,T.L., *et al.* (2006) *Cancer Res.*, **66**, 4339–4348.
Rajkumar,T., Stamp,G.W., Hughes,C.M. and Gullick,W.J. (1996a) *Clin. Mol. Pathol.*, **49**, M199–M202.
Rajkumar,T., Stamp,G.W., Pandha,H.S., Waxman,J. and Gullick,W.J. (1996b) *J. Pathol.*, **179**, 381–385.
Reschke,M., Mihic-Probst,D., van der Horst,E.H., Knyazev,P., Wild,P.J., Hutterer,M., Meyer,S., Dummer,R., Moch,H. and Ullrich,A. (2008) *Clin. Cancer Res.*, **14**, 5188–5197.
Rüther,U. (1982) *Nucleic Acids Res.*, **10**, 5765–5772.
Samuelson,P., Hansson,M., Ahlborg,N., Andreoni,C., Götz,F., Bachi,T., Nguyen,T.N., Binz,H., Uhlén,M. and Ståhl,S. (1995) *J. Bacteriol.*, **177**, 1470–1476.
Schmidt,M.M. and Wittrup,K.D. (2009) *Mol. Cancer Ther.*, **8**, 2861–2871.
Schoeberl,B., Pace,E.A., Fitzgerald,J.B., *et al.* (2009) *Sci. Signal*, **2**, ra31.
Sergina,N.V., Rausch,M., Wang,D., Blair,J., Hann,B., Shokat,K.M. and Moasser,M.M. (2007) *Nature*, **445**, 437–441.
Stove,C. and Bracke,M. (2004) *Clin. Exp. Metastasis*, **21**, 665–684.
Tanner,B., Hasenclever,D., Stern,K., *et al.* (2006) *J. Clin. Oncol.*, **24**, 4317–4323.
Tolmachev,V., Orlova,A., Nilsson,F.Y., Feldwisch,J., Wennborg,A. and Abrahmsén,L. (2007) *Expert Opin. Biol. Ther.*, **7**, 555–568.
Tolmachev,V., Friedman,M., Sandström,M., Eriksson,T.L., Rosik,D., Hodik,M., Ståhl,S., Frejd,F.Y. and Orlova,A. (2009) *J. Nucl. Med.*, **50**, 274–283.
Tolmachev,V., Rosik,D., Wållberg,H., Sjöberg,A., Sandström,M., Hansson,M., Wennborg,A. and Orlova,A. (2010) *Eur. J. Nucl. Med. Mol. Imaging*, **37**, 613–622.
Tran,T.A., Rosik,D., Abrahmsén,L., Sandström,M., Sjöberg,A., Wållberg,H., Ahlgren,S., Orlova,A. and Tolmachev,V. (2009) *Eur. J. Nucl. Med. Mol. Imaging*, **36**, 1864–1873.
VanAntwerp,J.J. and Wittrup,K.D. (2000) *Biotechnol. Prog.*, **16**, 31–37.
Wernérus,H. and Ståhl,S. (2004) *Biotechnol. Appl. Biochem.*, **40**, 209–228.